

SCALAR GLUONS AND DIRAC GLUINOS AT THE LHC*

S.Y. CHOI

Department Physics and RIPC, Chonbuk National University
Jeonju 561-756, Korea

J. KALINOWSKI

Faculty of Physics, University of Warsaw
Hoża 69, 00-681 Warsaw, Poland
and
CERN, Theoretical Physics, 1211 Geneva 23, Switzerland

J.M. KIM

Physikalisches Institut and Bethe CPT, Universität Bonn
Nussallee 12, 53115 Bonn, Germany

E. POPENDA

Institute of Theoretical Physics, Karlsruhe Institute of Technology
Kaiserstrasse 12, 76131 Karlsruhe, Germany

(Received October 29, 2009)

The hybrid $N = 1/N = 2$ supersymmetric model predicts scalar gluons (sgluons) as SUSY partners of the Dirac gluino. Their strikingly distinct phenomenology at the CERN Large Hadron Collider is discussed.

PACS numbers: 12.60.Jv, 14.80.Ly

1. Introduction

Among many propositions for the beyond the Standard Model (SM) physics, supersymmetry (SUSY) is generally considered most elegant and respected. It can accommodate or explain some of the outstanding problems of the SM. In fact, this is the only mathematically consistent UV completion of the SM that stabilizes the gap between electroweak and Planck scales.

* Presented by J. Kalinowski at the XXXIII International Conference of Theoretical Physics, "Matter to the Deepest", Ustroń, Poland, September 11–16, 2009 and at the 9th Hellenic School and Workshops on Elementary Particle Physics and Gravity, Corfu, Greece, August 30–September 6, 2009.

It provides the gauge coupling unification, radiative electroweak symmetry breaking, a candidate for dark matter (DM), offers new ideas on the matter-antimatter asymmetry *etc.*

The simplest $N = 1$ supersymmetric extension calls for each SM particle a sparticle that differs in spin by half a unit. The Lagrangian must be supplemented by SUSY breaking terms that keep unseen superpartners out of the current experimental reach while retaining all goodies of the model: renormalizability and perturbatively stable hierarchy of scales. With ever improving experimental constraints on SUSY breaking parameters, mainly from flavor and Higgs physics, the model building of successful SUSY breaking scenarios becomes more and more difficult.

However, the successes of supersymmetry do not rely on its simplest realization. In fact, non-minimal realizations may ameliorate some of the above problems. For example, Dirac gauginos (in contrast to Majorana in $N = 1$) forbid some of the couplings and may lead to additional suppression of loop contributions with gauginos in flavor-changing processes. Such scenarios can be based on D -term supersymmetry breaking models [1, 2] or continuous R -symmetries [3].

A Dirac gaugino requires additional fermionic degrees of freedom. They can be provided by adding chiral super-multiplets in the adjoint representations of the corresponding gauge group, as realised in $N = 2$ SUSY [4]. When extending to $N = 2$, the additional supersymmetry also requires the introduction of mirror matter superfields. In order to avoid chirality problems the $N = 2$ mirror (s)fermions have to be assumed to be heavy. Thus effectively we consider a hybrid model that expands to $N = 2$ only in the gaugino sector [5].

Here we will present elements of the phenomenology of the scalar partner of the Dirac gluino (sgluon), as worked out in a recent paper [6]; see also [7]. For an independent analysis of sgluons at the LHC, we refer to Ref. [8].

2. Basics of the $N = 1/N = 2$ hybrid model

If gluinos are seen at the LHC one of the main experimental goals will be to verify if they are Majorana or Dirac fermions. To address properly this issue a theoretical model is needed that allows a smooth Dirac/Majorana transition, as for example the hybrid model constructed in Ref. [5].

In $N = 1$ gluinos are Majorana fields with two degrees of freedom to match gluons in the color-octet vector super-multiplet. To provide the two additional degrees of freedom for Dirac fields, the usual $N = 1$ gluon/gluino $\{g^a, \tilde{g}^a\}$ super-multiplet $W_{3\alpha}^a = \tilde{g}_\alpha^a + D^a \theta_\alpha + (\sigma^{\mu\nu})_\alpha^\beta \theta_\beta G_{\mu\nu}^a + \dots$ ($a = 1, \dots, 8$) is supplemented by an additional $N = 1$ color-octet chiral super-multiplet $\Phi^a = \sigma^a + \sqrt{2}\theta^\alpha \tilde{g}'_\alpha{}^a + \theta\theta F^a$ of extra gluinos \tilde{g}'^a and scalar σ^a fields to form

a vector hyper-multiplet of $N = 2$ SUSY. Similarly, the electroweak sector, not to be discussed here, is supplemented by additional $SU(2)_L$ and $U(1)_Y$ super-multiplets [9].

2.1. Dirac/Majorana gluinos

Standard \tilde{g} and new gluinos \tilde{g}' couple minimally to the gluon field

$$\mathcal{L}_{\text{SQCD}} \ni g_s \text{Tr} \left(\bar{\tilde{g}} \gamma^\mu [g_\mu, \tilde{g}] + \bar{\tilde{g}'} \gamma^\mu [g_\mu, \tilde{g}'] \right), \tag{1}$$

as required by the gauge symmetry. Here g_s denotes the QCD coupling, the fields $g_\mu, \tilde{g}, \tilde{g}'$ are color-octet matrices (*e.g.* for the gluon $g_\mu = \frac{1}{\sqrt{2}} \lambda^a g_\mu^a$ with the Gell-Mann matrices λ^a); \tilde{g} and \tilde{g}' are two 4-component Majorana spinor fields. Quark and squark fields interact only with the standard gluino,

$$\mathcal{L}_{\text{SQCD}} \ni -g_s \left(\bar{q}_L \tilde{g} \tilde{q}_L - \bar{q}_R \tilde{g} \tilde{q}_R + \text{h.c.} \right), \tag{2}$$

since only their mirror partners (assumed to be heavy) couple to \tilde{g}' , as required by $N = 2$ SUSY.

Soft supersymmetry breaking generates masses for the gluino fields \tilde{g} and \tilde{g}' ,

$$\mathcal{M}_g = \begin{pmatrix} M_3 & M_3^D \\ M_3^D & M_3' \end{pmatrix}. \tag{3}$$

Diagonal terms are induced by the individual Majorana mass parameters M_3 and M_3' while an off-diagonal term corresponds to the Dirac mass. It can arise from the D -term, $\int d^2\theta \frac{\sqrt{2}}{M_0} W'^\alpha W_{3\alpha}^a \Phi^a + \text{h.c.}$ When a hidden sector spurion field W'_α gets a vacuum expectation value, $\langle W'_\alpha \rangle = D' \theta_\alpha$, the Dirac mass is generated, $M_3^D = D'/M_0$.

Diagonalization of (3) gives rise to two Majorana mass eigenstates, \tilde{g}_1 and \tilde{g}_2 , with masses m_1 and m_2 . There are two limiting cases of interest: in the limit $M_3' \rightarrow \pm\infty$ the standard Majorana gluino is recovered; in the limit of vanishing Majorana mass parameters M_3 and M_3' with $M_3^D \neq 0$, the mixing is maximal and the two Majorana gluino states are degenerate. One can draw a smooth path interpolating these two limiting cases by introducing an auxiliary parameter $y \in [-1, 0]$ and parameterizing $M_3' = y M_3^D / (1 + y)$, $M_3 = -y M_3^D$. With $M_3^D = m_{\tilde{g}_1}$ kept fixed, the parameter y allows for a continuous transition from $y = -1$, where the standard limit is reached with one Majorana gluino (the second being infinitely heavy), to $y = 0$ that corresponds to two degenerate Majorana fields combined to a Dirac gluino

$$\tilde{g}_D = \tilde{g}_R + \tilde{g}'_L. \tag{4}$$

The phenomenology of Dirac gluinos is characteristically different from Majorana. The detailed discussion can be found in Ref. [5], from which we borrow an example for illustration. Fig. 1 shows the partonic cross-sections

$q\bar{q}' \rightarrow \tilde{q}\tilde{q}'^*$ (left) and $qq' \rightarrow \tilde{q}\tilde{q}'$ (right) for different-flavor squark production, in both cases mediated by the gluino t -channel exchange, plotted as a function of a Dirac/Majorana control parameter y (for partonic center-of-mass energy $\sqrt{s} = 2000$ GeV, $m_{\tilde{q}} = 500$ GeV and $m_{\tilde{g}_1} = 600$ GeV). We see that $\sigma[q\bar{q}' \rightarrow \tilde{q}_L\tilde{q}'_R^*]$ and $\sigma(qq' \rightarrow \tilde{q}_L\tilde{q}'_L) = \sigma(qq' \rightarrow \tilde{q}_R\tilde{q}'_R)$ are non-zero in the Majorana limit but vanish in the Dirac, while $\sigma[q\bar{q}' \rightarrow \tilde{q}_L\tilde{q}'_L^*] = \sigma[q\bar{q}' \rightarrow \tilde{q}_R\tilde{q}'_R^*]$ and $\sigma(qq' \rightarrow \tilde{q}_L\tilde{q}'_R)$ are non-zero for any y and reach the same values in both limits. For equal-flavor quark–antiquark scattering the additional gluino s -channel exchange must be added to the t -channel exchange diagrams.

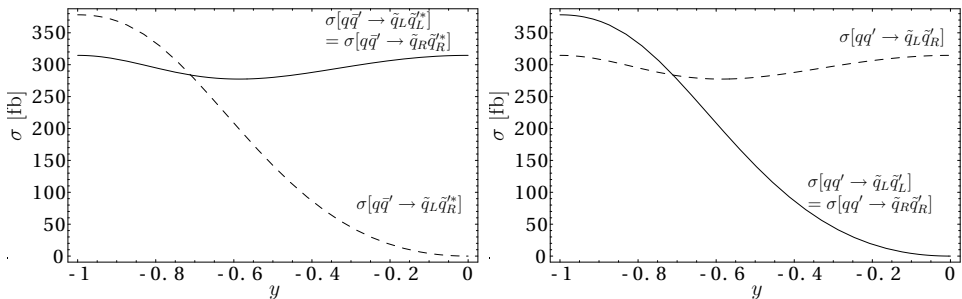


Fig. 1. Cross-sections for different-flavor squark production in $q\bar{q}' \rightarrow \tilde{q}\tilde{q}'^*$ (left) and $qq' \rightarrow \tilde{q}\tilde{q}'$ (right) as a function of the Dirac/Majorana control parameter y .

2.2. Sgluons

The gluinos \tilde{g}^a are accompanied by a color-octet complex scalar field σ^a . In parallel to the case of degenerate Majorana gluinos combined to the Dirac, the real and imaginary components of the scalar field σ will be assumed degenerate with the sgluon mass denoted by M_σ [6].

Although sgluons are R -parity even, they cannot be singly produced at tree level in gluon–gluon or quark–antiquark collision. This is so because they couple only in pairs to gluons, $\sigma\sigma^*g$ and $\sigma\sigma^*gg$, as required by the gauge symmetry, and singly only to Dirac gluino pairs via the Yukawa-type gauge interaction

$$\mathcal{L}_{\tilde{g}_D\tilde{g}_D\sigma} = -\sqrt{2}i g_s f^{abc} \tilde{g}_{DL}^a \tilde{g}_{DR}^b \sigma^c + \text{h.c.}, \quad (5)$$

where f^{abc} are the $SU(3)_C$ structure constants. It is interesting to note that even the loop-induced σgg coupling due to gluino exchange vanish as a consequence of Bose symmetry since the coupling is even in momentum space but odd, $\sim f^{abc}$, in color space¹.

¹ Since the sgluon couples only to two different Majorana gluinos, Eq. (5), while gluons always couple to the same pair, Eq. (1), the coupling of the octet sgluon to any number of gluons via the gluino loop is forbidden.

When SUSY is broken spontaneously, the Dirac gluino mass generates, via the super-QCD D -term, a scalar coupling between σ and squark pair [1]

$$\mathcal{L}_{\sigma\tilde{q}\tilde{q}} = -g_s M_3^D \sigma^a \frac{\lambda_{ij}^a}{\sqrt{2}} \sum_q (\tilde{q}_{Li}^* \tilde{q}_{Lj} - \tilde{q}_{Ri}^* \tilde{q}_{Rj}) + \text{h.c.} \quad (6)$$

Note that the L and R squarks contribute with opposite signs. Since squarks couple to gluons and quarks, the loop diagrams with squark/gluino lines, Fig. 2, generate σgg and $\sigma q\bar{q}$ couplings. The interaction Lagrangian however, Eq. (6), implies that all L - and R -squark contributions to the couplings come with opposite signs so that they cancel each other for mass degenerate squarks. In addition, the quark–antiquark coupling is suppressed by the quark mass as evident from general chirality rules.

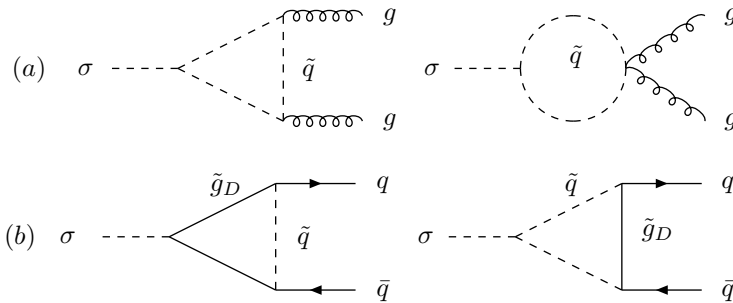


Fig. 2. Generic diagrams for the effective σgg (a) and $\sigma q\bar{q}$ (b) vertices with squark/gluino loops.

3. Sgluon production and decays at the LHC

Since sgluons have a large color charge they might be more copiously produced than squarks at the LHC. In addition, they have quite spectacular decay modes, as discussed below.

3.1. Sgluon decays

Sgluons can decay into a variety of different channels that include gluinos, squarks, gluons and quarks. At tree level the σ particles can decay only to a pair of Dirac gluinos \tilde{g}_D or into a pair of squarks (if kinematically open),

$$\Gamma[\sigma \rightarrow \tilde{g}_D \tilde{g}_D] = \frac{3\alpha_s M_\sigma}{4} \beta_{\tilde{g}} (1 + \beta_{\tilde{g}}^2), \quad (7)$$

$$\Gamma[\sigma \rightarrow \tilde{q}_a \tilde{q}_a^*] = \frac{\alpha_s |M_3^D|^2}{4M_\sigma} \beta_{\tilde{q}_a}, \quad (8)$$

where $\beta_{\tilde{g}, \tilde{q}_a}$ are the velocities of \tilde{g}, \tilde{q}_a ($a = L, R$). If $M_\sigma < 2M_{\tilde{g}_D}, 2m_{\tilde{q}}$, one or both of these sparticles can be virtual. Squarks and gluinos will further cascade to SM particles and LSP.

Decays into gluon or quark–antiquark pairs can proceed only via loop-induced couplings. In the case of no L/R squark mixing² the decay widths take the form

$$\Gamma(\sigma \rightarrow gg) = \frac{5\alpha_s^3}{384\pi^2} \frac{|M_3^D|^2}{M_\sigma} \left| \sum_q [\tau_{\tilde{q}_L} f(\tau_{\tilde{q}_L}) - \tau_{\tilde{q}_R} f(\tau_{\tilde{q}_R})] \right|^2, \quad (9)$$

$$\Gamma(\sigma \rightarrow q\bar{q}) = \frac{9\alpha_s^3}{128\pi^2} \frac{|M_3^D|^2 m_q^2}{M_\sigma} \beta_q [(M_\sigma^2 - 4m_q^2) |\mathcal{I}_S|^2 + M_\sigma^2 |\mathcal{I}_P|^2], \quad (10)$$

where $\tau_{\tilde{q}_{L,R}} = 4m_{\tilde{q}_{L,R}}^2/M_\sigma^2$ and $f(\tau)$ is the standard function from a squark circulating in the loop [10], while the effective scalar (\mathcal{I}_S) and pseudoscalar (\mathcal{I}_P) $\sigma q\bar{q}$ couplings are given by ($i = S, P$)

$$\mathcal{I}_i = \int_0^1 dx \int_0^{1-x} dy [w_i (C_L^{-1} - C_R^{-1}) + z_i (D_L^{-1} - D_R^{-1})]. \quad (11)$$

In the above expression $w_S = 1 - x - y$, $w_P = 1$, $z_S = (x + y)/9$, $z_P = 0$, and the squark/gluino denominators are ($a = L, R$)

$$C_a = (x + y) |M_3^D|^2 + (1 - x - y)m_{\tilde{q}_a}^2 - xyM_\sigma^2 - (x + y)(1 - x - y)m_q^2,$$

$$D_a = (1 - x - y) |M_3^D|^2 + (x + y)m_{\tilde{q}_a}^2 - xyM_\sigma^2 - (x + y)(1 - x - y)m_q^2.$$

Because of the chirality, decays to quark–antiquark pairs are suppressed by the quark mass. Therefore, the decays into top quark pairs will dominate. In addition, both loop-induced decays $\sigma \rightarrow gg$ and $\sigma \rightarrow q\bar{q}$ are absent if L and R squarks are degenerate. Therefore, squarks with substantial mixing (mostly top squarks) will contribute to the decay widths.

The hierarchy between the tree-level and loop-induced decay modes depends on the values of various soft breaking parameters. The tree-level, two-body decays of Eqs (7), (8) will dominate if they are kinematically allowed. Well above all thresholds the partial width into gluinos always dominates: it grows $\propto M_\sigma$ since the supersymmetric $\sigma\tilde{g}\tilde{g}$ coupling is dimensionless, while the partial width into squarks asymptotically scales like $1/M_\sigma$ due to dimensionfull SUSY-breaking $\sigma\tilde{q}\tilde{q}^*$ coupling.

² If \tilde{q}_L and \tilde{q}_R of a given flavor mix, the subscripts L, R have to be replaced by 1, 2 labeling the squark mass eigenstates, and the contribution from this flavor is suppressed by the factor $\cos(2\theta_q)$.

When the above decay channels are shut kinematically, even for small L – R squark mass splitting the loop-induced sgluon decays into two gluons, and to a $t\bar{t}$ pair if kinematically allowed, always dominate over tree-level off-shell four-body decays $\sigma \rightarrow \tilde{g}q\bar{q}\tilde{\chi}$ and $\sigma \rightarrow q\bar{q}\tilde{\chi}\tilde{\chi}$. Increasing the gluino mass increases the $\sigma\tilde{q}\tilde{q}^*$ coupling. As a result, the partial width into two gluons (due to pure squark loops) increases, while the $t\bar{t}$ partial width (due to mixed squark–gluino loops) decreases since the increase of the $\sigma\tilde{q}\tilde{q}$ couplings is over-compensated by the gluino mass dependence of the propagators.

The above qualitative features are verified numerically in Fig. 3, where the branching ratios for σ decays are shown for two different squark/gluino mass hierarchies. Plots are done for moderate mass splitting between the L and R squarks of the five light flavors, and somewhat greater for soft breaking \tilde{t} masses: $m_{\tilde{q}_R} = 0.95m_{\tilde{q}_L}$, $m_{\tilde{t}_L} = 0.9m_{\tilde{q}_L}$, $m_{\tilde{t}_R} = 0.8m_{\tilde{q}_L}$ with the off-diagonal element of the squared \tilde{t} mass matrix $X_t = m_{\tilde{q}_L}$; the gluino is taken to be a pure Dirac state, *i.e.* $m_{\tilde{g}} = |M_3^D|$.

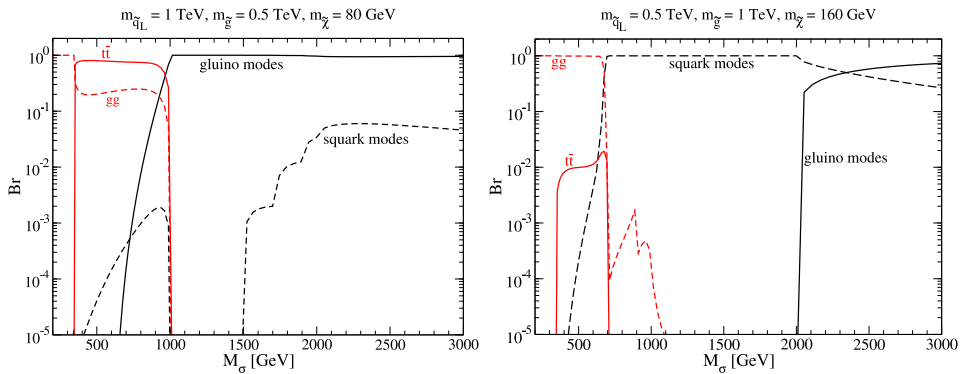


Fig. 3. Branching ratios for σ decays, for $m_{\tilde{q}_L} = 2m_{\tilde{g}} = 1$ TeV (left) and $m_{\tilde{g}} = 2m_{\tilde{q}_L} = 1$ TeV (right).

3.2. Sgluon production at the LHC

The signatures for single σ production are potentially very exciting. They can be produced singly in gluon–gluon collisions via squark loops since the production via $q\bar{q}$ annihilation is negligible for light incoming quarks. The partonic cross-section is given by

$$\hat{\sigma}[gg \rightarrow \sigma] = \frac{\pi^2}{M_\sigma^3} \Gamma(\sigma \rightarrow gg), \quad (12)$$

where the partial width for $\sigma \rightarrow gg$ decays is given in Eq. (9). The expected cross-section for single σ production can be quite large at the designed LHC energy, of the order 100 fb. Its dependence on the sgluon mass is shown by

the curves (c) and (d) in Fig. 4 (with the LO CTEQ6L parton densities [11]). In the scenario of the right frame of Fig. 3, the single σ cross-section can exceed the σ -pair production cross-section for $M_\sigma \sim 1$ TeV (solid curve (c)); the dashed one (d) is for the benchmark point SPS1a' [12] with the gluino mass interpreted as a Dirac mass. Since the latter scenario has a somewhat smaller gluino mass, it generally leads to smaller cross-sections for single σ production.

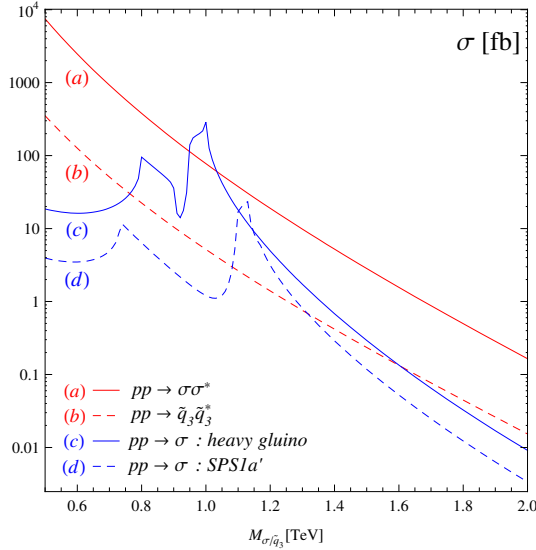


Fig. 4. Cross-sections for σ -pair [and \tilde{q}_3 -pair] production (lines (a) and (b)), as well as for single σ production (lines (c) and (d)), at the LHC. The curve (c) is for the mass parameters as in Fig. 3 (right), while the dashed (d) for the mSUGRA benchmark point SPS1a'.

It would be very exciting to observe the sgluon as an s -channel resonance. This, however, will not be easy since (a) the 2-gluon decay channel must be discriminated from large background, (b) large production cross-section in the gluon fusion implies diminished decay rates to other channels, which in addition do not allow a direct reconstruction of M_σ . Detailed experimental simulations are needed to see if the single σ production can be detected as a resonance above the SM and SUSY backgrounds.

Sgluons can also be pair-produced in $q\bar{q}$ and gg processes at tree-level,

$$\sigma[q\bar{q} \rightarrow \sigma\sigma^*] = \frac{4\pi\alpha_s^2}{9s} \beta_\sigma^3, \tag{13}$$

$$\sigma[gg \rightarrow \sigma\sigma^*] = \frac{15\pi\alpha_s^2\beta_\sigma}{8s} \left[1 + \frac{34}{5} \frac{M_\sigma^2}{s} - \frac{24}{5} \left(1 - \frac{M_\sigma^2}{s} \right) \frac{M_\sigma^2}{s} L_\sigma \right], \tag{14}$$

where \sqrt{s} is the invariant parton-parton energy, M_σ and β_σ are the mass and center-of-mass velocity of the σ particle, and $L_\sigma = \beta_\sigma^{-1} \log(1 + \beta_\sigma)/(1 - \beta_\sigma)$. The cross-section for σ -pair production at LHC, $pp \rightarrow \sigma\sigma^*$, is shown by the solid curve (a) in Fig. 4 for the σ -mass range between 500 GeV and 2 TeV. With values from several picobarn downwards, a sizable $\sigma\sigma^*$ event rate can be generated. As expected, due to large color charge of the sgluon, the $\sigma\sigma^*$ cross-section exceeds stop or sbottom-pair production (dashed line (b)), mediated by a set of topologically equivalent Feynman diagrams, by more than an order of magnitude.

With the exception of $\sigma \rightarrow gg$, all the σ decays give rise to signatures that should easily be detectable. Most spectacular ones come from $\sigma \rightarrow \tilde{g}\tilde{g}$ decay followed by the gluino decays giving at the end at least four hard jets and two invisible neutralinos as LSP's. The σ -pair production then generates final states with a minimum of four LSP's and eight jets with transverse momenta distributions markedly different from the corresponding standard gluino or squark production with the same mass configurations [6]. Other interesting final states are four top squarks $\tilde{t}_1\tilde{t}_1\tilde{t}_1^*\tilde{t}_1^*$, which can dominate if $m_{\tilde{q}} \lesssim m_{\tilde{g}}$ and L - R mixing is significant in the stop sector, and $\tilde{q}\tilde{q}^*\tilde{g}\tilde{g}$ if $M_\sigma > 2m_{\tilde{g}} \gtrsim 2m_{\tilde{q}}$. They also give rise to four LSP's in the final state and a large number of hard jets.

The $gg + gg$ and $t\bar{t} + t\bar{t}$ final states, which can be the dominant modes if the two-body decays into squarks and gluinos are kinematically shut, might also allow the direct kinematic reconstruction of M_σ . Preliminary analyses of the $gg + gg$ channel show that pairing the four hardest jets in the central region of rapidity with no missing E_T could reveal the signal and provide a means to reconstruct the σ mass directly [13]. In addition, the observation of $t\bar{c}\bar{t}c$ final states would signal a substantial mixing in the up-type squark sector.

4. Summary

Models with Dirac gauginos offer an interesting alternative to the standard SUSY scenario. They predict the existence of scalar particles in the adjoint representation of the gauge groups. The color-octet scalars, sgluons, can be copiously produced at the LHC since they carry large color charge. Their signatures at the LHC are distinctly different from the usual topologies. Depending on the assumed scenario of masses and SUSY breaking parameters, either multi-jet final states with high sphericity and large missing transverse momentum are predicted, or four top quarks and/or four gluon jets should be observed in 2σ production. In the latter the sgluon mass could be reconstructed directly. If the mass splitting between L and R squarks is not too small, loop-induced single σ production may also have

a sizable cross-section. It remains to be checked by detailed experimental simulations whether such a single resonant σ production is detectable on the large SM and SUSY background.

We thank Peter Zerwas and Manuel Drees for a fruitful collaboration. Work supported in parts by the Korea Research Foundation Grant KRF-2008-521-C00069, the Polish Ministry of Science and Higher Education Grant N N202 230337, and the EC Programmes MRTN-CT-2006-035505 “Tools and Precision Calculations for Physics Discoveries at Collider” and MTKD-CT-2005-029466 “Particle Physics and Cosmology: The Interface”. J.K. is grateful to the Theory Division for the hospitality extended to him at CERN.

REFERENCES

- [1] P.J. Fox, A.E. Nelson, N. Weiner, *J. High Energy Phys.* **0208**, 035 (2002).
- [2] Y. Nomura, D. Poland, B. Tweedie, *Nucl. Phys.* **B745**, 29 (2006).
- [3] L.J. Hall, L. Randall, *Nucl. Phys.* **B352**, 289 (1991); G.D. Kribs, E. Poppitz, N. Weiner, *Phys. Rev.* **D78**, 055010 (2008).
- [4] P. Fayet, *Nucl. Phys.* **B113**, 135 (1976); **B149**, 137 (1979); F. del Aguila, M. Dugan, B. Grinstein, L.J. Hall, G.G. Ross, P.C. West, *Nucl. Phys.* **B250**, 225 (1985); L. Álvarez-Gaumé, S.F. Hassan, *Fortsch. Phys.* **45**, 159 (1997).
- [5] S.Y. Choi, M. Drees, A. Freitas, P.M. Zerwas, *Phys. Rev.* **D78**, 095007 (2008).
- [6] S.Y. Choi, M. Drees, J. Kalinowski, J.M. Kim, E. Popenza, P.M. Zerwas, *Phys. Lett.* **B672**, 246 (2009).
- [7] S.Y. Choi, M. Drees, J. Kalinowski, J.M. Kim, E. Popenza, P.M. Zerwas, *Acta Phys. Pol. B* **40**, 1947 (2009); J.M. Kim, talk at the 15th Int. Symposium on Particles, Strings and Cosmology Pascos2009, DESY, Hamburg; E. Popenza, talk at the GRD Terascale Workshop, Heidelberg 2009.
- [8] T. Plehn, T.M.P. Tait, *J. Phys. G* **36**, 075001 (2009).
- [9] For a recent discussion of dark matter with Dirac and Majorana neutralinos, see G. Belanger, K. Benakli, M. Goodsell, C. Moura, A. Pukhov, *JCAP* **0908**, 027 (2009).
- [10] J.F. Gunion, H.E. Haber, *Nucl. Phys.* **B278**, 449 (1986).
- [11] J. Pumplin, D.R. Stump, J. Huston, H.L. Lai, P.M. Nadolsky, W.K. Tung, *J. High Energy Phys.* **0207**, 012 (2002).
- [12] J.A. Aguilar-Saavedra *et al.*, *Eur. Phys. J.* **C46**, 43 (2006).
- [13] A. Renaud, Sgluons at the LHC: A First Look, talk at the GRD Terascale Workshop, Heidelberg 2009; See also C. Kilic, S. Schumann, M. Son, *J. High Energy Phys.* **0904**, 128 (2009).